JOURNAL OF GUIDANCE, CONTROL, AND DYNAMICS
Vol. 32, No. 6, November–December 2009

Engineering Notes

Simplified Singularity Avoidance Using Variable-Speed Control Moment Gyroscope Null Motion

Jay McMahon* and Hanspeter Schaub†
University of Colorado at Boulder, Boulder, Colorado 80309-0431

DOI: 10.2514/1.45433

I. Introduction

SINGULARITY avoidance in variable-speed control moment gyroscope (VSCMG) systems can require significant computation to determine null motion steering commands. This paper presents a less complicated method of determining appropriate null motion steering laws while achieving similar performance with current, more complicated, methods.

Control moment gyroscope (CMG) clusters, which are often used for spacecraft attitude control, can encounter singular gimbal-angle configurations for which a general three-dimensional torque cannot be produced. Such singularities can be overcome through a variety of methods, such as those presented in [1,2]. Another option to help avoid singularities is to use VSCMG devices, which allow a CMG device to vary its wheel speed, and thus produce a torque of about two orthogonal axes (wheel spin and transfer axis) [3–5]. A VSCMG cluster will not encounter gimbal locks (singular gimbal-angle configurations) due to the reaction wheel (RW) modes. If all the CMG torque axes lie in a plane, then one of the RW control axes will point apart from this CMG torque plane. Thus, a VSCMG cluster can always produce the required torque of a chosen attitude control law without encountering temporary small attitude errors, as the CMG singularity is avoided. However, using RW modes to drive through the CMG singular configuration requires significant RW motor torques, which is not power effective [6]. Using the null space of the VSCMG system wisely can enable the system to avoid this singular CMG situation while completing the required control maneuvers. The extra RW control modes of the VSCMG allow for greater effectiveness to rearrange the gimbal angles away from the CMG singularity [7]. This increased null space of the VSCMG devices can also be used to create novel combined attitude and energy storage devices [8–10]. Here, the rotor speed can be spun up during sunlit portions of the orbit to store energy without changing the spacecraft attitude. Then, during a shaded orbit region, the rotors can be spun down using the VSCMG null space to extract this energy again.

VSCMG steering laws lead to a simple condition that maps the desired rotor accelerations and gimbal rates into the required attitude control torque. The null space of this mapping is exploited by Schaub and Junkins using a gradient-based method to drive the gimbal angles away from a CMG singularity [7]. The condition number of the mapping matrix is used as the singularity index. Yoon and Tsiotras analyzed the CMG singularities of VSCMG devices in [11] and provided a small modification to the gradient-based null space proposed in [7]. The advantage of this modification is that stability of the singularity avoidance can be analytically guaranteed. However, this new null space steering law requires particular control of both the wheel speed and the gimbal rate, whereas the earlier method only required gimbal-angle motion. The reduced actuation requirements are a benefit because this makes it easier for the null space to be used to implement auxiliary objects, such as power storage demands or returning the wheel speeds to their original values and avoiding long-term rotor speed drift. Lee et al. presented, in [12], a general formulation to develop optimal null space VSCMG steering laws to avoid a CMG singularity. Their method can account for higher-order CMG cost function sensitivities and provide analytical stability guarantees. However, as with the method by Yoon and Tsiotras, the VSCMG steering law dictates both rotor speed and gimbal-angle changes. If reduced to a simple first-order form, their general formulation can be shown to be a generalization of the earlier methods discussed in [7,11].

Many VSCMG null space steering methods have developed their formulation around the attitude regulation problem. The algebraic null space formulation often becomes significantly more complex if an attitude tracking problem is considered. This Technical Note investigates a simplified CMG singularity measure for which the performance is equivalent to the previously published methods, but it is implemented using a substantial reduction in complexity. In particular, considering an attitude tracking problem does not lead to an increase in complexity. The developments are performed, and numerically simulated, using the optimal steering formulation by Lee et al. [12]. However, the presented results could also be easily applied to the VSCMG null space steering law presented by Yoon and Tsiotras [11].

II. Steering Law Overview

Figure 1 illustrates the gimbal frame coordinate system $\mathcal{G}$: $\{\hat{\boldsymbol{g}}_s, \hat{\boldsymbol{g}}_t, \hat{\boldsymbol{g}}_g\}$ used to describe the time-varying orientation of the VSCMG relative to the spacecraft body $\mathcal{B}$. The gimbal rate $\dot{\gamma}_i$ is applied about the body-fixed axis $\hat{\boldsymbol{g}}_{g_i}$, whereas the rotor speed motor causes angular accelerations $\dot{\Omega}_i$ about the spin axis $\hat{\boldsymbol{g}}_{s_i}$. All VSCMG steering laws for both attitude regulation and tracking application lead to a control condition of the form [3–5,13]:

$$[Q]\dot{\boldsymbol{\eta}} = \mathbf{L}_r \tag{1}$$

$$[Q] = [D_0 \quad D] \tag{2}$$

$$\dot{\boldsymbol{\eta}} = \begin{bmatrix} \dot{\boldsymbol{\Omega}} \\ \dot{\gamma} \end{bmatrix} \tag{3}$$

Here, $[D_0]$ and $[D]$ are $3 \times N$ matrices, with N being the number of VSCMGs in the system. The projection matrix $[Q]$ is therefore a $3 \times 2N$ matrix that maps the VSCMG control states to the required $N \times 1$ control vector $\mathbf{L}_r$. This Technical Note follows the notation setup in [5,7], which also provide expressions for $\mathbf{L}_r$ for attitude regulation and tracking control formulations. Finally, the parameters $\dot{\boldsymbol{\Omega}}$ and $\dot{\boldsymbol{\gamma}}$ are the $N \times 1$ wheel speed and gimbal rate vectors, respectively.

The wheel speed rate control matrix $[D_0]$ is formulated by [5]

$$[D_0] = [\cdots \quad \hat{\mathbf{g}}_{s_i} \quad J_{s_i} \quad \cdots] \tag{4}$$

Received 13 May 2009; revision received 3 August 2009; accepted for publication 3 August 2009.

*Graduate Research Assistant, Aerospace Engineering Sciences, 431 UCB.

†Associate Professor, H. Joseph Smead Fellow, Aerospace Engineering Sciences Department, 431 UCB. Associate Fellow Member AIAA.

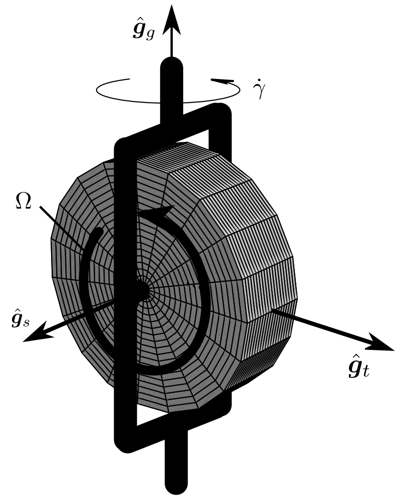

Fig. 1 Variable-speed CMG coordinate frame illustration.

and the gimbal rate control matrix $[D]$ for the reference attitude tracking problem is given by [5]

$$[D] = \left\{ \cdots \; J_{s_i}\left[\hat{\mathbf{g}}_{t_i}\left(\Omega_i + \tfrac{1}{2}\omega_{s_i}\right) + \tfrac{1}{2}\omega_{t_i}\hat{\mathbf{g}}_{s_i}\right] - \tfrac{1}{2}J_{t_i}(\omega_{t_i}\hat{\mathbf{g}}_{s_i} + \omega_{s_i}\hat{\mathbf{g}}_{t_i}) + J_{g_i}(\omega_{t_i}\hat{\mathbf{g}}_{s_i} - \omega_{s_i}\hat{\mathbf{g}}_{t_i}) + \tfrac{1}{2}(J_{s_i} - J_{t_i})(\hat{\mathbf{g}}_{s_i}\hat{\mathbf{g}}_{t_i}^T\boldsymbol{\omega}_r + \hat{\mathbf{g}}_{t_i}\hat{\mathbf{g}}_{s_i}^T\boldsymbol{\omega}_r) \cdots \right\} \tag{5}$$

where $\boldsymbol{\omega}_r$ is the reference trajectory angular velocity. The $\mathcal{G}$-frame axes can be grouped into a matrix such that each axis forms a column. For example, using the transverse axes $\hat{\boldsymbol{g}}_{t_i}$ we find

$$[G_t] = [\,\hat{\mathbf{g}}_{t_1} \quad \cdots \quad \hat{\mathbf{g}}_{t_i} \quad \cdots \quad \hat{\mathbf{g}}_{t_N}\,] \tag{6}$$

The same notation can be used to create $[G_s]$ and $[G_g]$ matrices. J_s, J_t, and J_g are the combined wheel and gimbal structure moments of inertia in the spin, transverse, and gimbal directions, respectively. The projection of the spacecraft body angular velocity $\boldsymbol{\omega} = \boldsymbol{\omega}_{\mathcal{B}/\mathcal{N}}$ onto the ith gimbal frame $\mathcal{G}$ yields

$$\boldsymbol{\omega} = \omega_{s_i}\hat{\boldsymbol{g}}_{s_i} + \omega_{t_i}\hat{\boldsymbol{g}}_{t_i} + \omega_{g_i}\hat{\boldsymbol{g}}_{g_i} \tag{7}$$

If examining the attitude regulation problem, the VSCMG steering law projection matrix $[D]$ can be simplified from Eq. (5) by setting $\omega_r = 0$ and dropping nonworking terms to become [5]

$$[D]_{\text{reg}} = \{\cdots \quad \hat{\mathbf{g}}_{t_i} \quad [J_{s_i}(\Omega_i + \omega_{s_i}) - J_{t_i}\omega_{s_i}] \quad \cdots\} \tag{8}$$

Note that both versions of $[D]$ depend on the gimbal angles γ_i through the dependence on $\hat{\boldsymbol{g}}_{s_i}$, $\hat{\boldsymbol{g}}_{t_i}$, ω_{s_i}, and ω_{t_i}, and on the rotor spin rates Ω_i. A further simplification of $[D]$ is typically made in recognizing that the $J_{t_i}\omega_{s_i}$ term is very small compared with the other terms due to the size of the inertias; therefore, the typical form for regulator control is

$$[Q] = [\,D_0 \quad D_1\,] \tag{9}$$

where

$$[D_1] = [\cdots \quad \hat{\mathbf{g}}_{t_i} \quad J_{s_i} \quad (\Omega_i + \omega_{s_i}) \quad \cdots] \tag{10}$$

Whereas, the $[Q]$ matrix will never be singular, it is possible for the $[D]$ or $[D_1]$ matrices to become singular. In this case, the VSCMG cannot fully employ the CMG mode, and some RW modes must be employed to produce the required control torque $\mathbf{L}_r$. The goal of the VSCMG null motion steering law is to keep the $[D]$ or $[D_1]$ matrices (tracking or regulation cases) full rank at all times.

Solving the control constraint in Eq. (1) results in the spacecraft executing the desired stabilizing motion. But, due to the fact that a typical four VSCMG system has a five-dimensional null space, there are infinite ways to solve for the steering command $\dot{\boldsymbol{\eta}}$. Typically, the desired solution is executed primarily with the CMG modes using a weighted minimum norm inverse of Eq. (1). To ensure that the CMG mode can be used at all times, the control solution must consider CMG singularity avoidance using the VSCMG control modes.

III. Variable-Speed Control Moment Gyroscope Optimal Steering Law

Lee et al. presented, in [12], an optimal VSCMG null space steering law formulation to avoid the CMG singular configuration. This formulation relied on a CMG singularity measure V that must be minimized while keeping the VSCMG steering commands $\dot{\boldsymbol{\eta}}$ small. This section provides a brief overview of Lee's method, including second-order sensitivities. If the singularity measure V has a complex form, then the null space steering law formulation quickly increases in complexity. This Technical Note provides first- and second-order singularity sensitivities for regulation and tracking problems using both the $[D]$ matrix and the simplified singularity measure.

The singularity avoidance cost function used to derive Lee's optimal steering is [12]

$$J(\dot{\boldsymbol{\eta}}) = V(\boldsymbol{\eta} + \dot{\boldsymbol{\eta}}\Delta t) + \tfrac{1}{2}\dot{\boldsymbol{\eta}}^T W \dot{\boldsymbol{\eta}} + \tfrac{1}{2}(\dot{\boldsymbol{\eta}} - \dot{\boldsymbol{\eta}}_d)^T Z (\dot{\boldsymbol{\eta}} - \dot{\boldsymbol{\eta}}_d) \tag{11}$$

where $\dot{\boldsymbol{\eta}}_d$ is a vector of preferred gimbal and wheel speed rates, and

$$\dot{\boldsymbol{\eta}}_d = \frac{\boldsymbol{\eta}_d - \boldsymbol{\eta}}{\Delta t} \tag{12}$$

where $\boldsymbol{\eta}_d$ is a vector of desired values for the gimbal angles and wheel speeds.

The first term V in the cost function J is the singularity avoidance cost. The second term is the weighted cost for the control effort, and the final term is the weighted cost for deviated state values. Typically, only the wheel speeds are weighted in the third term, which allows the gimbals to vary in any way without impacting the cost function through this term. This is assumed to be the case for the remainder of this paper.

The Hessian matrix $\bar{H}$ and the gradient vector $\mathbf{g}$ are defined as

$$\bar{H} = \equiv \Delta t^2 V''(\boldsymbol{\eta}) = \Delta t^2 \begin{bmatrix} \frac{\partial^2 V}{\partial \Omega^2} & \frac{\partial^2 V}{\partial \Omega \partial \gamma} \\ \frac{\partial^2 V}{\partial \gamma \partial \Omega} & \frac{\partial^2 V}{\partial \gamma^2} \end{bmatrix} \tag{13}$$

and

$$\mathbf{g}(\boldsymbol{\eta}) = \begin{bmatrix} \mathbf{g}_\Omega \\ \mathbf{g}_\gamma \end{bmatrix} = \Delta t V'(\boldsymbol{\eta}) = \Delta t \begin{bmatrix} \frac{\partial V}{\partial \Omega} & \frac{\partial V}{\partial \gamma} \end{bmatrix}^T \tag{14}$$

where $\mathbf{g}_\Omega$ and $\mathbf{g}_\gamma \in \mathbb{R}^N$ are the partitions of the gradient matrix. Using these definitions of the Hessian and the gradient matrices, and ignoring the higher-order terms, the singularity avoidance cost is approximated as

$$V(\boldsymbol{\eta} + \dot{\boldsymbol{\eta}}\Delta t) \simeq V(\boldsymbol{\eta}) + \mathbf{g}^T\dot{\boldsymbol{\eta}} + \tfrac{1}{2}\dot{\boldsymbol{\eta}}^T\bar{H}\,\dot{\boldsymbol{\eta}} \tag{15}$$

Using this framework, the optimal steering law is solved to be

$$\begin{bmatrix} \dot{\boldsymbol{\Omega}} \\ \dot{\boldsymbol{\gamma}} \end{bmatrix} = \hat{S}\hat{Q}^+\mathbf{L}_r + (\hat{S}\hat{Q}^+\hat{S}^T - \hat{H}^{-1})\begin{bmatrix} \hat{\mathbf{g}}_\Omega \\ \hat{\mathbf{g}}_\gamma \end{bmatrix} \tag{16}$$

where

$$\hat{S} = \hat{H}^{-1}Q^T, \qquad \hat{Q}^+ = (Q\hat{H}^{-1}Q^T)^{-1} \tag{17}$$

Here, the modified Hessian and gradient matrices are defined as

$$\hat{H} = \bar{H} + W + Z \tag{18}$$

$$\hat{\mathbf{g}} = \begin{bmatrix} \hat{\mathbf{g}}_\Omega \\ \hat{\mathbf{g}}_\gamma \end{bmatrix} = \begin{bmatrix} \mathbf{g}_\Omega - Z_\Omega\dot{\Omega}_d \\ \mathbf{g}_\gamma \end{bmatrix} \tag{19}$$

It should be noted that this optimal steering law is very similar to that proposed in [7] for singularity avoidance and constant wheel speeds.

The main difference is that the optimal steering law uses the second-order derivatives for V and requires both $\dot{\Omega}_i$ and $\dot{\gamma}_i$ to perform the desired null motion, whereas [7] only uses the first-order derivatives and the gimbal rates $\dot{\gamma}_i$. The choice of the singularity index V results in varying algebraic complexities of the optimal steering law formulation. Furthermore, it is beneficial to not require both specific $\dot{\gamma}_i$ and $\dot{\Omega}_i$ to avoid a CMG singularity. This makes it simpler to implement other objectives, such as nominally constant rotor speeds or power extraction requirements, using the VSCMG null motion.

IV. Singularity Avoidance

Although the VSCMG configuration cannot become singular like a CMG system ($[Q]$ is always full rank) [3], avoiding the geometrically singular CMG configuration $\hat{\boldsymbol{g}}_{t_i}$ in the same plane for the regulation case is still desirable. In general, it is more efficient to steer with the CMG mode as much as possible [6]. Furthermore, the rotor speeds will saturate much sooner than the gimbals when producing a given torque; therefore, smart VSCMG control systems attempt to keep the wheel speeds near the nominal values.

Mathematically, the singular CMG situation that needs to be avoided is when the $\hat{\boldsymbol{g}}_{t_i}$ axis become coplanar. The gimbal rates $\dot{\gamma}_i$ produce a torque about the $\hat{\boldsymbol{g}}_{t_i}$ axis. Thus, if these only span a two-dimensional space, then the CMG control modes cannot produce a general three-dimensional vector. This is seen directly for the regulation case in the $[D_1]$ matrix; the columns depend directly on the transverse axes.

The same argument can be used for attitude tracking problem with the full $[D]$ matrix. Although there are other terms present that are proportional to $\hat{\boldsymbol{g}}_{s_i}$, the dominant terms are still the gyroscopic term proportional to $J_{s_i}\Omega_i$. If the transverse axes become coplanar, then torques out of plane could still be produced. But, because the other terms are small in comparison to the $J_{s_i}\Omega_i$ term, the required motion will be an undesirable method of producing the torque.

In any case, a VSCMG steering law not only implements the required torque, but it also has some null motion to avoid the singularity situation. For the regulation case, [7] continuously minimizes the condition number of the $[D_1]$ matrix. The condition number of a matrix κ is defined as the ratio of the largest to the smallest singular values of the chosen $3 \times N$ matrix:

$$\kappa = \frac{\sigma_1}{\sigma_3} \tag{20}$$

For the tracking case, one would use the condition number of the $[D]$ matrix. Likewise, these condition numbers can be used as the CMG singularity V function in the optimal steering law developed by Lee et al. [12].

This Technical Note proposes to always use the condition number of the $[G_t]$ matrix in place of the $[D]$ or $[D_1]$ matrices condition numbers. This makes intuitive sense; the situation that is to be avoided is the transverse axes $\hat{\boldsymbol{g}}_{t_i}$ becoming coplanar, and thus the loss of full three-dimensional CMG control authority. If the condition number of $[G_t]$ is kept small, then the matrix is being kept at full rank, and therefore the transverse axes are spanning three-dimensional space instead of becoming coplanar. Furthermore, using $[G_t]$ works for the regulation or tracking case, unlike $[D]$ or $[D_1]$, and therefore does not require reworking the steering law for each specific case.

Note the following subtle issue with using the condition number of $[G_t]$ versus that of $[D]$ or $[D_1]$. The later matrices depend on the rotor speeds Ω_i. Thus, the VSCMG null motion can modify the rotor speeds to minimize the condition number κ. This ability is lost with the simplified singularity measure using the condition number of $[G_t]$ only. However, as is illustrated in the enclosed numerical simulations, as long as the rotor speeds are kept apart from zero, the resulting CMG avoidance performance is essentially equivalent to those of using the more complex condition number formulation of the $[D_1]$ and $[D]$ matrices.

A second-order form of Lee's optimal steering law is examined that requires the first and second partial derivatives of the condition number with respect to both the gimbal angles and the wheel speeds. The first partial derivatives are defined as

$$\frac{\partial \kappa}{\partial \Omega_i} = \frac{1}{\sigma_3}\frac{\partial \sigma_1}{\partial \Omega_i} - \frac{\sigma_1}{\sigma_3^2}\frac{\partial \sigma_3}{\partial \Omega_i} \tag{21}$$

$$\frac{\partial \kappa}{\partial \gamma_i} = \frac{1}{\sigma_3}\frac{\partial \sigma_1}{\partial \gamma_i} - \frac{\sigma_1}{\sigma_3^2}\frac{\partial \sigma_3}{\partial \gamma_i} \tag{22}$$

where $i = 1, \ldots, N$. The partial derivatives of the singular values of a given matrix $[A]$ are given by [14]

$$\frac{\partial \sigma_j}{\partial \Omega_i} = \mathbf{u}_j^T \frac{\partial [A]}{\partial \Omega_i}\mathbf{v}_j \tag{23}$$

$$\frac{\partial \sigma_j}{\partial \gamma_i} = \mathbf{u}_j^T \frac{\partial [A]}{\partial \gamma_i}\mathbf{v}_j \tag{24}$$

where the singular value decomposition of $[A]$ is

$$[A] = [U][\Sigma][V]^T$$

$\mathbf{u}_j$ is the jth column of $[U]$, and $\mathbf{v}_j$ is the jth column of $[V]$.

The second partial derivatives of κ can be obtained by applying the chain rule to Eqs. (21) and (22) to get

$$\frac{\partial^2 \kappa}{\partial \Omega_i \partial \Omega_j} = \frac{1}{\sigma_3}\frac{\partial^2 \sigma_1}{\partial \Omega_i \partial \Omega_j} - \frac{1}{\sigma_3^2}\frac{\partial \sigma_1}{\partial \Omega_i}\frac{\partial \sigma_3}{\partial \Omega_j} - \frac{1}{\sigma_3^2}\left(\frac{\partial \sigma_3}{\partial \Omega_i}\frac{\partial \sigma_1}{\partial \Omega_j} + \sigma_1 \frac{\partial^2 \sigma_3}{\partial \Omega_i \partial \Omega_j}\right) + \frac{2\sigma_1}{\sigma_3^3}\frac{\partial \sigma_3}{\partial \Omega_i}\frac{\partial \sigma_3}{\partial \Omega_j} \tag{25}$$

$$\frac{\partial^2 \kappa}{\partial \Omega_i \partial \gamma_j} = \frac{\partial^2 \kappa}{\partial \gamma_i \partial \Omega_j} = \frac{1}{\sigma_3}\frac{\partial^2 \sigma_1}{\partial \Omega_i \partial \gamma_j} - \frac{1}{\sigma_3^2}\frac{\partial \sigma_1}{\partial \Omega_i}\frac{\partial \sigma_3}{\partial \gamma_j} - \frac{1}{\sigma_3^2}\left(\frac{\partial \sigma_3}{\partial \Omega_i}\frac{\partial \sigma_1}{\partial \gamma_j} + \sigma_1 \frac{\partial^2 \sigma_3}{\partial \Omega_i \partial \gamma_j}\right) + \frac{2\sigma_1}{\sigma_3^3}\frac{\partial \sigma_3}{\partial \Omega_i}\frac{\partial \sigma_3}{\partial \gamma_j} \tag{26}$$

$$\frac{\partial^2 \kappa}{\partial \gamma_i \partial \gamma_j} = \frac{1}{\sigma_3}\frac{\partial^2 \sigma_1}{\partial \gamma_i \partial \gamma_j} - \frac{1}{\sigma_3^2}\frac{\partial \sigma_1}{\partial \gamma_i}\frac{\partial \sigma_3}{\partial \gamma_j} - \frac{1}{\sigma_3^2}\left(\frac{\partial \sigma_3}{\partial \gamma_i}\frac{\partial \sigma_1}{\partial \gamma_j} + \sigma_1 \frac{\partial^2 \sigma_3}{\partial \gamma_i \partial \gamma_j}\right) + \frac{2\sigma_1}{\sigma_3^3}\frac{\partial \sigma_3}{\partial \gamma_i}\frac{\partial \sigma_3}{\partial \gamma_j} \tag{27}$$

The second partials of the singular values can then be determined by differentiating equations (23) and (24),

$$\frac{\partial^2 \sigma_j}{\partial \Omega_i \partial \Omega_k} = \mathbf{u}_j^T \frac{\partial^2 [A]}{\partial \Omega_i \partial \Omega_k}\mathbf{v}_j \tag{28}$$

$$\frac{\partial^2 \sigma_j}{\partial \Omega_i \partial \gamma_k} = \frac{\partial^2 \sigma_j}{\partial \gamma_i \partial \Omega_k} = \mathbf{u}_j^T \frac{\partial^2 [A]}{\partial \Omega_i \partial \gamma_k}\mathbf{v}_j \tag{29}$$

$$\frac{\partial^2 \sigma_j}{\partial \gamma_i \partial \gamma_k} = \mathbf{u}_j^T \frac{\partial^2 [A]}{\partial \gamma_i \partial \gamma_k}\mathbf{v}_j \tag{30}$$

For a given matrix $[A]$ (which will be $[D]$, $[D_1]$, or $[G_t]$), the partial derivatives will have the form

$$\frac{\partial [A]}{\partial \gamma_i} = [\mathbf{0} \quad \cdots \quad \mathbf{0} \quad \boldsymbol{\chi}_i \quad \mathbf{0} \quad \cdots \quad \mathbf{0}] \tag{31}$$

$$\frac{\partial [A]}{\partial \Omega_i} = [\mathbf{0} \quad \cdots \quad \mathbf{0} \quad \boldsymbol{\psi}_i \quad \mathbf{0} \quad \cdots \quad \mathbf{0}] \tag{32}$$

$$\frac{\partial^2 [A]}{\partial \Omega_i \Omega_j} = 0 \quad \forall\ i,\ j \tag{33}$$

$$\frac{\partial^2[A]}{\partial\Omega_i\gamma_j} = \frac{\partial^2[A]}{\partial\gamma_i\Omega_j} = [\mathbf{0} \quad \cdots \quad \mathbf{0} \quad \boldsymbol{\xi}_i \quad \mathbf{0} \quad \cdots \quad \mathbf{0}] \tag{34}$$

$$\frac{\partial^2[A]}{\partial\gamma_i\gamma_j} = [\mathbf{0} \quad \cdots \quad \mathbf{0} \quad \boldsymbol{\phi}_i \quad \mathbf{0} \quad \cdots \quad \mathbf{0}] \tag{35}$$

The derivation for each of the three matrices is shown in the following subsections. It is made clear that determining the singularity avoidance controls is much simpler for $[G_t]$ than either $[D]$ or $[D_1]$.

A. $[D_1]$ Matrix Condition Number

For the attitude regulation control case, [7] presents the partial derivative of $[D_1]$ with respect to γ_i as

$$\boldsymbol{\chi}_i = -\hat{\mathbf{g}}_{s_i} J_{s_i}(\Omega_i + \omega_{s_i}) + \hat{\mathbf{g}}_{t_i} J_{s_i}\omega_{t_i} \tag{36}$$

Likewise, the partial derivative of $[D_1]$ with respect to Ω_i is

$$\boldsymbol{\psi}_i = \hat{\mathbf{g}}_{t_i} J_{s_i} \tag{37}$$

The second partial derivative of $[D_1]$ with respect to γ_i and Ω_i is

$$\boldsymbol{\xi}_i = \begin{cases} 0 & i \neq j \\ -\hat{\mathbf{g}}_{s_i} J_{s_i} & i = j \end{cases} \tag{38}$$

The second partial derivative of $[D_1]$ with respect to γ_i is

$$\boldsymbol{\phi}_i = \begin{cases} 0 & i \neq j \\ -\hat{\mathbf{g}}_{t_i} J_{s_i}(\Omega_i + 2\omega_{s_i}) - \hat{\mathbf{g}}_{s_i} J_{s_i}\omega_{t_i} & i = j \end{cases} \tag{39}$$

B. $[D]$ Matrix Condition Number

For the reference attitude tracking control case, the first partial derivative of $[D]$ with respect to γ_i is

$$\begin{aligned}\boldsymbol{\chi}_i = {} & J_{s_i}(-\Omega_i\hat{\mathbf{g}}_{s_i} - \omega_{s_i}\hat{\mathbf{g}}_{s_i} + \omega_{t_i}\hat{\mathbf{g}}_{t_i}) + J_{t_i}(\omega_{s_i}\hat{\mathbf{g}}_{s_i} - \omega_{t_i}\hat{\mathbf{g}}_{t_i}) \\ & + (J_{s_i} - J_{t_i})(\hat{\mathbf{g}}_{t_i}\hat{\mathbf{g}}_{t_i}^T\boldsymbol{\omega}_r - \hat{\mathbf{g}}_{s_i}\hat{\mathbf{g}}_{s_i}^T\boldsymbol{\omega}_r)\end{aligned} \tag{40}$$

The partial derivative of $[D]$ with respect to Ω_i is

$$\boldsymbol{\psi}_i = \hat{\mathbf{g}}_{t_i} J_{s_i} \tag{41}$$

The second partial derivatives of $[D]$ with respect to γ_i and Ω_i are

$$\boldsymbol{\xi}_i = \begin{cases} 0 & i \neq j \\ -\hat{\mathbf{g}}_{s_i} J_{s_i} & i = j \end{cases} \tag{42}$$

The second partial derivative of $[D]$ with respect to γ_i is

$$\boldsymbol{\phi}_i = \begin{cases} 0 & i \neq j \\ 2J_{s_i}(-\frac{1}{2}\Omega_i\hat{\mathbf{g}}_{t_i} - \omega_{s_i}\hat{\mathbf{g}}_{t_i} - \omega_{t_i}\hat{\mathbf{g}}_{s_i}) & \\ +2J_{t_i}(\omega_{t_i}\hat{\mathbf{g}}_{s_i} + \omega_{s_i}\hat{\mathbf{g}}_{t_i}) & \\ -2(J_{s_i} - J_{t_i})(\hat{\mathbf{g}}_{s_i}\hat{\mathbf{g}}_{t_i}^T\boldsymbol{\omega}_r + \hat{\mathbf{g}}_{t_i}\hat{\mathbf{g}}_{s_i}^T\boldsymbol{\omega}_r) & i = j \end{cases} \tag{43}$$

C. $[G_t]$ Matrix Condition Number

For both the attitude regulation and tracking cases, the first partial derivatives of $[G_t]$ have the very simple form

$$\boldsymbol{\chi}_i = -\hat{\mathbf{g}}_{s_i} \tag{44}$$

$$\boldsymbol{\psi}_i = \mathbf{0} \tag{45}$$

Likewise, the second partial derivatives have the simple forms

$$\boldsymbol{\xi}_i = \mathbf{0} \tag{46}$$

and

$$\boldsymbol{\phi}_i = \begin{cases} 0 & i \neq j \\ -\hat{\mathbf{g}}_{t_i} & i = j \end{cases} \tag{47}$$

The functional form of using the condition number of $[G_t]$ is much simpler than those of the $[D_1]$ or $[D]$ matrices. Furthermore, it is important to note that the wheel speeds are not needed to determine the null motion steering commands for singularity avoidance, unlike with the other cost functions. The effectiveness of this simple CMG singularity measure is demonstrated in the following numerical simulations.

V. Simulation Results

A test simulation is used to illustrate the performance of the singularity avoidance using $[G_t]$ for a tracking case. For this simulation, the satellite properties are the same as were used by Schaub and Junkins [7] and are reproduced in Table 1. This simulation uses the full nonlinear acceleration-based equations of motion developed in [5]. A subservo gimbal acceleration controller (with feedforward term) is used to implement the VSCMG gimbal rate $\dot{\gamma}_i$ commands from the optimal steering law.

In the following simulation, the optimal steering law proposed by Lee et al. [12] is used and the control parameters are shown in Table 2. An additional VSCMG state goal is implemented in which any rotor speeds Ω_i should return gradually back to their original states. The attitude control goal is to track a reference rotation while continuously avoiding a CMG singularity. The reference trajectory is created assuming the satellite is commanded to constantly point at a fixed spot on the Earth's surface. This is executed by rotating the spacecraft about its first body axis $\hat{\boldsymbol{b}}_1$ in order to always keep the body z axis pointing at the desired location.

Figure 2 shows attitude error between the body quaternion and the reference trajectory quaternion, and Fig. 3 shows the body axis angular velocities along with the reference trajectory commands. The difference between the actual and reference trajectories is very small. Also recall that using any method of singularity avoidance results in the same tracking performance because the singularity avoidance motion is in the null space and therefore does not apply any net torques to the spacecraft. The differences shown in the three illustrated cases are due to the different gimbal rate commands resulting in slightly different gimbal acceleration-based implementations.

Figures 4 and 5 show the VSCMG wheel speeds and gimbal angles, respectively, for the controller using the condition number of $[D]$ and $[G_t]$. Different singularity avoidance methods are expected to show different motions for each individual VSCMG component.

Table 1 Spacecraft properties

Parameter	Value
I_{s_1}	$15,053\ \text{kg}\cdot\text{m}^2/\text{s}$
I_{s_2}	$6,510\ \text{kg}\cdot\text{m}^2/\text{s}$
I_{s_3}	$11,122\ \text{kg}\cdot\text{m}^2/\text{s}$
N	4
θ	54.75 deg
J_s	$0.70\ \text{kg}\cdot\text{m}^2$
J_t	$0.35\ \text{kg}\cdot\text{m}^2$
J_g	$0.35\ \text{kg}\cdot\text{m}^2$

Table 2 Control parameters

Parameter	Value
$\Omega_i(t_0)$	628 rad/s
$\gamma_i(t_0)$	$[45 \quad -45 \quad 45 \quad -45]$ deg
Δt	0.01 s
Ω_d	628 rad/s
W_γ	$0.8I_{N\times N}$
W_Ω	$0.008I_{N\times N}$
Z_Ω	$0.008I_{N\times N}$
$\mathbf{K}$	$2\ \text{kg}\cdot\text{m}^2/\text{s}$
$[P]$	$30I_{N\times N}\ \text{kg}\cdot\text{m}^2/\text{s}$

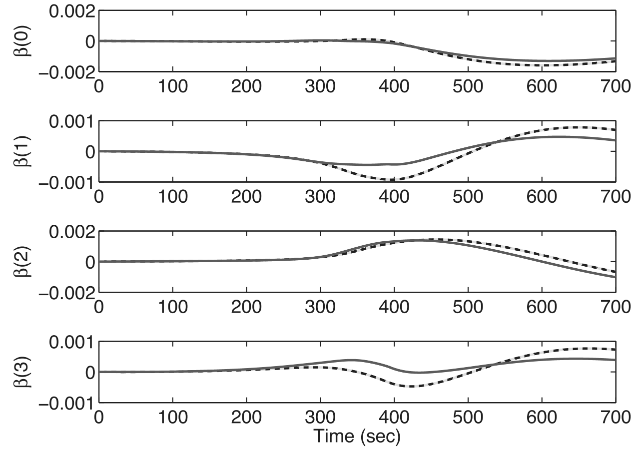

Fig. 2 Quaternion attitude errors between body and reference frame. The results using the $[G_t]$ cost function (dashed lines) are directly on top of the results using the $[D]$ cost function (solid lines). The other solid line illustrates the case without any CMG avoidance null motion.

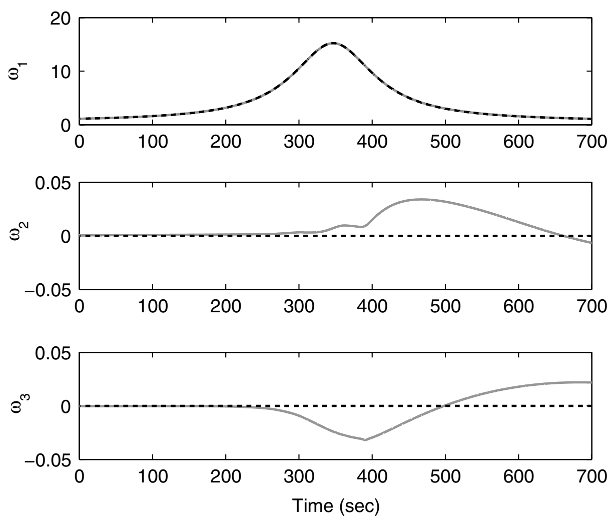

Fig. 3 Spacecraft (solid line) and reference (dashed line) angular velocities in mrad/s.

However, this case shows that the results of using the different singularity avoidance measurements show almost identical motion for every component of the system. This implies that the methods result in nearly identical null motion commands, and therefore the considerably more complex computations to use $[D]$ made little difference in the final closed-loop performance.

Finally, Fig. 6 shows the comparison of the condition numbers for the three different singularity control methods. It is evident that the

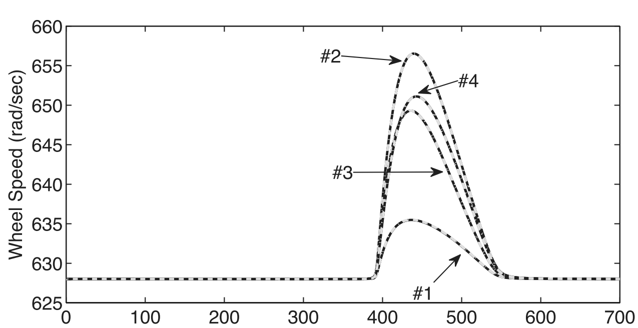

Fig. 4 Time histories of the four VSCMG wheel speeds Ω_i. All four wheels show nearly identical speed profiles using $[G_t]$ or $[D]$; the results of both appear as the dashed line.

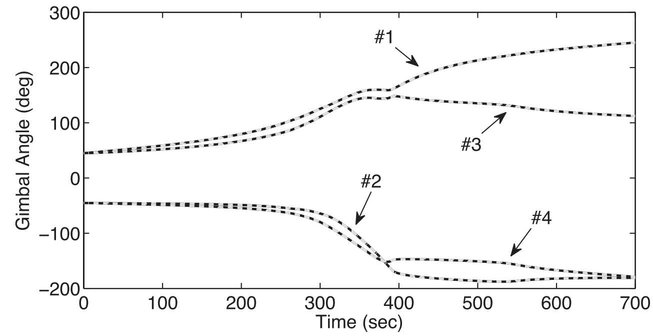

Fig. 5 Time histories of the four individual VSCMG gimbal angles γ_i. All four wheels show nearly identical orientations using $[G_t]$ or $[D]$; the results of both appear as the dashed line.

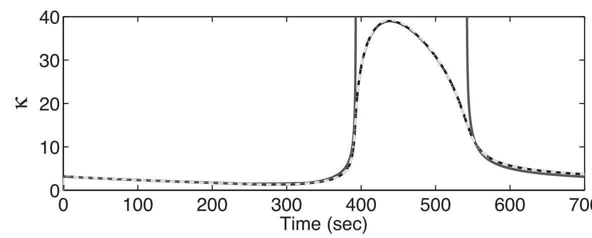

Fig. 6 Condition numbers of using the optimal controller with $[D]$ or $[G_t]$ appear as the dashed line. The solid line illustrates the performance of the first-order gradient method of [7] using the condition number of $[D]$.

two optimal steering methods using either the condition number of $[D]$ or $[G_t]$ have nearly identical performances. The difference is only 0.62% at the peak of κ at 450 s, too small to be of practical consequence. During the time frame when the condition number increases, the wheel speeds also change in Fig. 4; this is when the VSCMG cluster is near the CMG singularity. Both singularity avoidance methods work appropriately to reduce the condition number and then to return the rotor speeds back to their nominal values. The third simulation contrasts the optimal VSCMG steering law performance to the simple first-order gradient method proposed in [7]. The condition number is also reduced back to a small value, but after growing first to a much larger value of approximately 82,000. This comparison is interesting in that the optimal steering law minimizing the condition number of $[G_t]$ also only requires the gimbal rates in the resulting null space motion.

VI. Conclusions

This Technical Note introduces a simple method to implement a CMG singularity avoidance null motion for a VSCMG control system. This method is based on tracking the range of the transverse axes instead of the rank of the VSCMG steering control projection matrix. The new approach does not require any knowledge of the rotor speeds in order to create singularity avoidance null motion steering commands. The performance using this simpler CMG singularity cost function is essentially identical to previously published methods, as is illustrated with a simple numerical simulation. The main benefit of this new method for CMG singularity avoidance using VSCMG devices is that the null motion commands are greatly simplified compared with previous methods.

References

[1] Nakamura, Y., and Hanafusa, H., "Inverse Kinematic Solutions with Singularity Robustness for Robot Manipulator Control," *Journal of Dynamic Systems, Measurement, and Control*, Vol. 108, No. 3, 1986, pp. 163–171.
doi:10.1115/1.3143764

[2] Leeghim, H., Bang, H., and Park, J.-O., "Singularity Avoidance of Control Moment Gyros by One-Step Ahead Singularity Index," *Acta*

Astronautica, Vol. 64, Nos. 9–10, May–June 2009, pp. 935–945.
doi:10.1016/j.actaastro.2008.11.004

[3] Schaub, H., Vadali, S. R., and Junkins, J. L., "Feedback Control Law for Variable Speed Control Moment Gyroscopes," *Journal of the Astronautical Sciences*, Vol. 45, No. 3, July–Sept. 1998, pp. 307–328.

[4] Ford, K. A., and Hall, C. D., "Flexible Spacecraft Reorientations Using Gimbaled Momentum Wheels," *Journal of the Astronautical Sciences*, Vol. 49, No. 3, 2001, pp. 421–441.

[5] Schaub, H., and Junkins, J., *Analytical Mechanics of Space Systems*, AIAA, Reston, VA, 2003.

[6] Lappas, V. J., Steyn, W. H., and Underwood, C. I., "Practical Results on the Development of a Control Moment Gyro Based Attitude Control System for Agile Small Satellites," AIAA/USU Small Satellite Conference, Utah State Univ., Paper SSC02-VI-4, Logan, UT, 12–15 Aug. 2002.

[7] Schaub, H., and Junkins, J. L., "Singularity Avoidance Using Null Motion and Variable Speed Control Moment Gyros," *Journal of Guidance, Control, and Dynamics*, Vol. 23, No. 1, Jan.–Feb. 2000, pp. 11–16.
doi:10.2514/2.4514

[8] Tsiotras, P., Shen, H., and Hall, C. D., "Satellite Attitude Control and Power Tracking with Energy/Momentum Wheels," *Journal of Guidance, Control, and Dynamics*, Vol. 24, No. 1, 2001, pp. 23–34.
doi:10.2514/2.4705

[9] Yoon, H., and Tsiotras, P., "Spacecraft Adaptive Attitude and Power Tracking with Variable Speed Control Moment Gyroscopes," *Journal of Guidance, Control, and Dynamics*, Vol. 25, No. 6, Nov.–Dec. 2002, pp. 1081–1090.
doi:10.2514/2.4987

[10] Yoon, H., and Tsiotras, P., "Singularity Analysis and Avoidance of Variable-Speed Control Moment Gyros, Part II: Power Constraint Case," Proceedings of the AIAA/AAS Astrodynamics Specialist Conference and Exhibit, AIAA Paper 2004-5208, 16–19 Aug. 2004.

[11] Yoon, H., and Tsiotras, P., "Singularity Analysis of Variable Speed Control Moment Gyros," *Journal of Guidance, Control, and Dynamics*, Vol. 27, No. 3, 2004, pp. 374–386.
doi:10.2514/1.2946

[12] Lee, H., Lee, I.-H., and Bang, H., "Optimal Steering Laws for Variable Speed Control Moment Gyros," AIAA Guidance, Navigation, and Control Conference and Exhibit, AIAA Paper 2005-6395, Aug. 2005.

[13] Richie, D. J., Lappas, V. J., and Prassinos, G., "A Practical Small Satellite Variable Speed Control Moment Gyroscope For Combined Energy Storage and Attitude Control," AIAA/AAS Astrodynamics Specialist Conference and Exhibit, AIAA Paper 2008-7503, 18–21 Aug. 2008.

[14] Junkins, J. L., and Kim, Y., *Introduction to Dynamics and Control of Flexible Structures*, AIAA Education Series, AIAA, Washington, D. C., 1993.